

Can We Trust the Transgenic Mouse? Insights from Computer Simulations

Joseph Tranquillo and Adhira Sunkara

Bucknell University, Lewisburg PA 17837, USA
jvt002@bucknell.edu
<http://www.facstaff.bucknell.edu/jvt002>

Abstract. Over the past several decades, the mouse has gained prominence in the cardiac electrophysiology literature as the animal model of choice. Using computer models of the mouse and human ECG, this paper is a step toward understanding when the mouse succeeds and fails to mimic functional changes resulting from disease states and drug interactions.

1 Introduction

The transgenic mouse has enjoyed a large share of the spotlight in the cardiovascular literature over the past decade, primarily due to the relative ease of genetic manipulation [1,2,3,4,5,6,7], and miniaturization of recording techniques [8,9,10]. These advances have enabled models of human disease to be studied in mice at spatial scales ranging from protein channels to the whole heart. At first glance, the mouse appears to be a scaled version of the human heart. For example, the mouse heart rate is approximately 10 times faster than in the human, while the Action Potential Duration (APD) and left ventricular wall thickness are approximately 10 times smaller [7,11]. On the other hand, some measures are comparable. At the organ level, the human and mouse fiber organization and anisotropic conduction patterns are similar [12,13]. At the tissue level, the resting length constants and conduction velocities [1,14,15] are similar. At the protein level, most ion channels are conserved across species [11].

It is because some properties are similar while others are scaled that calls into question the use of the mouse as a model of human disease. For example, as the mouse and human length constants are similar but the ventricular wall thicknesses are an order of magnitude different, the mouse may not supporting the same transmural APD gradients as the human [16,17]. Furthermore, the dominate repolarization current in the mouse is I_{to} and I_{sus} while in the human I_{Ks} and I_{Kr} rectify the transmembrane potential [11,18,19].

An ideal animal model would be similar to the human at all scales and measurements. Although some animal models approach this ideal (e.g. Porcine), they are typically costly. The second ideal animal model would be one that is perfectly scaled compared to the human. Some computational models may achieve this [20], but no animal models are available. In the absence or difficulty of using these two ideal animal models, the next option is the one that has been adopted by the field; an animal that can be modified to mimic the human.

Accepting that it is impractical to perfectly scale the mouse to the human, it is important to understand the limitations of the mouse model. Although a systematic study is possible using experimental models, it is more efficient to explore the limitations in a computer model. This paper is a first step toward creating such models. The Electrocardiogram (ECG) has been targeted because: 1) genetic mutations at the protein level can have an impact on the ECG. 2) simple simulations [21] may reproduce the impact of these mutations and 3) the mouse and human ECG have noticeably different morphologies [11,17,22,23].

2 Methods

2.1 Cellular Models

The ten Tusscher et al. [19] and Pandit et al. [18] ionic current models were used for human and mouse simulations respectively. Figure 1 is a comparison of epicardial action potentials and ionic currents for both models.

2.2 Cable Models

Ionically heterogeneous and spatially isotropic one dimensional monodomain ($dx = 0.01cm$, $\sigma = 1mS/cm$) cables were used to simulate the mouse and human left ventricular wall. The forward Euler ($dt = 2\mu s$) method was used for numerical integration. The profile of the human left ventricular wall was simulated by a $1.65cm$ cable divided into epicardial ($0 - 0.6cm$), M ($0.6 - 1.05cm$) and endocardial ($1.05 - 1.65cm$) regions [21]. The profile of the mouse left ventricular wall was simulated in a $0.2cm$ cable that was divided into epicardial ($0 - 0.1cm$) and endocardial ($0.1 - 0.2cm$) regions. Propagation in both cables was initiated by ten, supra-threshold current stimuli at the endocardial end of the cable. The pacing rate for the human was 1Hz while the mouse was 8Hz.

2.3 Computation of the Pseudo-electrocardiogram (pECG)

The pECG was computed as the extracellular potential (ϕ_e) generated by transmembrane currents (I_m) propagating down a cable surrounded by a large volume conductor ($\sigma_e = 6mS/cm$):

$$\phi_e = \frac{1}{4\pi\sigma_e} \int \frac{I_m}{r} dV$$

where r is the distance from the recording point to the current source I_m [24] and the reference electrode is at infinity. The current source is the sum of capacitive and ionic currents. In both mouse and human cables, the recording electrode was placed $1cm$ from the epicardium.

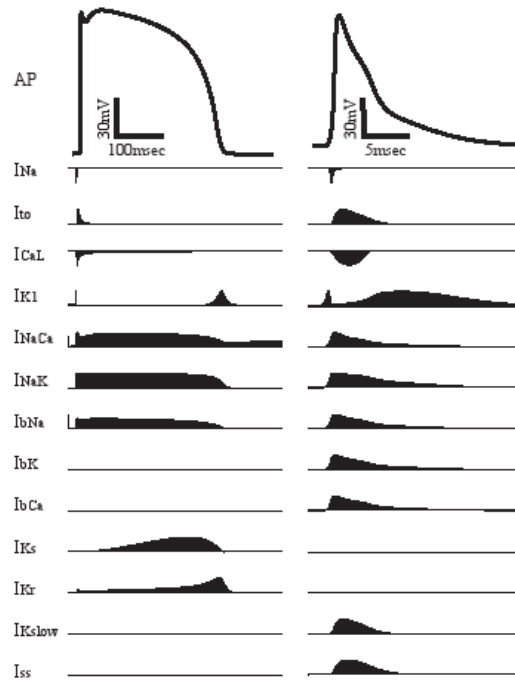


Fig. 1. Human (left) and Mouse (right) epicardial action potentials and currents

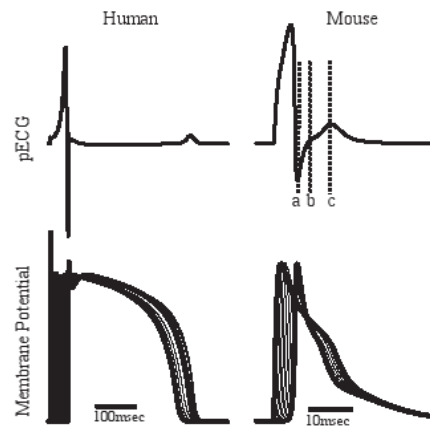


Fig. 2. Human pECG (left) and Mouse pECG (right). The mouse pECG was scored by: a) first deflection to minimum, b) minimum slope after a wave and before final deflection c) peak (or valley) of final deflection. For reference, bottom traces show the V_m time course of every $1mm$ and $200\mu m$ along the cable for the human and mouse respectively.

2.4 Simulation of Mutations

The maximum channel conductances were independently varied (both increased and decreased) for all currents shared by the two species (Figure 1). As I_{NaK} and I_{NaCa} do not play a large role in simple beat studies, we have omitted these currents. Brugada Syndrome was simulated by a modification of I_{Na} activation and inactivation profiles [25]. The impact of adding a human I_{Ks} and I_{Kr} to the mouse model was also explored.

2.5 Analysis of Results

All results were analyzed for the tenth paced beat. The normal mouse epicardial and endocardial APDs were 13.5 and 26.1msec respectively while the human epi, M and endo APDs were 270, 275 and 323msec respectively (-60mV crossings). The mouse Conduction Velocity (CV) was 41cm/s while the human CV=40.5cm/s (delays in -60mV crossings). CVs do not significantly change unless noted. As scoring of the mouse ECG has not been standardized, we have adopted the a , b , c notion (Figure 2) proposed by Danik et al. [22].

3 Results

3.1 Comparisons of Normal Mouse and Human pECG

The simulated Normal Human pECG (Figure 2) shows a narrow QRS (corresponding to conduction of depolarization from endocardium to epicardium), slight J-wave elevation (corresponding to rapid repolarization) followed by a long isopotential (corresponding to the action potential plateau) and finally the T-wave (due to complex repolarization timing from epicardium to endocardium and finally the mid-wall). The simulated mouse ECG also shows a QRS-like complex (a-wave) that like the human corresponds to depolarization across the wall from endocardium to epicardium. As the epicardium depolarizes, the voltage gradient reverses briefly, giving rise to the b-wave. The origin of the b-wave therefore appears to be similar to the J-wave in the human, although it may be exaggerated. The epicardium rapidly repolarizes before the endocardium (as in the human), giving rise to a second voltage gradient reversal and the c-wave. The origin of the b-wave therefore appears to be similar to the T-wave in the human.

3.2 Reduced I_{K1}

I_{K1} is a primary current in determining the resting membrane potential and underlies Andersen's syndrome. Blocking I_{K1} , raises the resting potential for both the mouse and the human (Figure 3A). In the human, the rise in resting potential partially inactivates Na^+ channels, leading to slower conduction and a broader QRS complex. Since all other currents are tuned to the original resting potential, a hyperpolarization follows repolarization that leads to a small non-zero

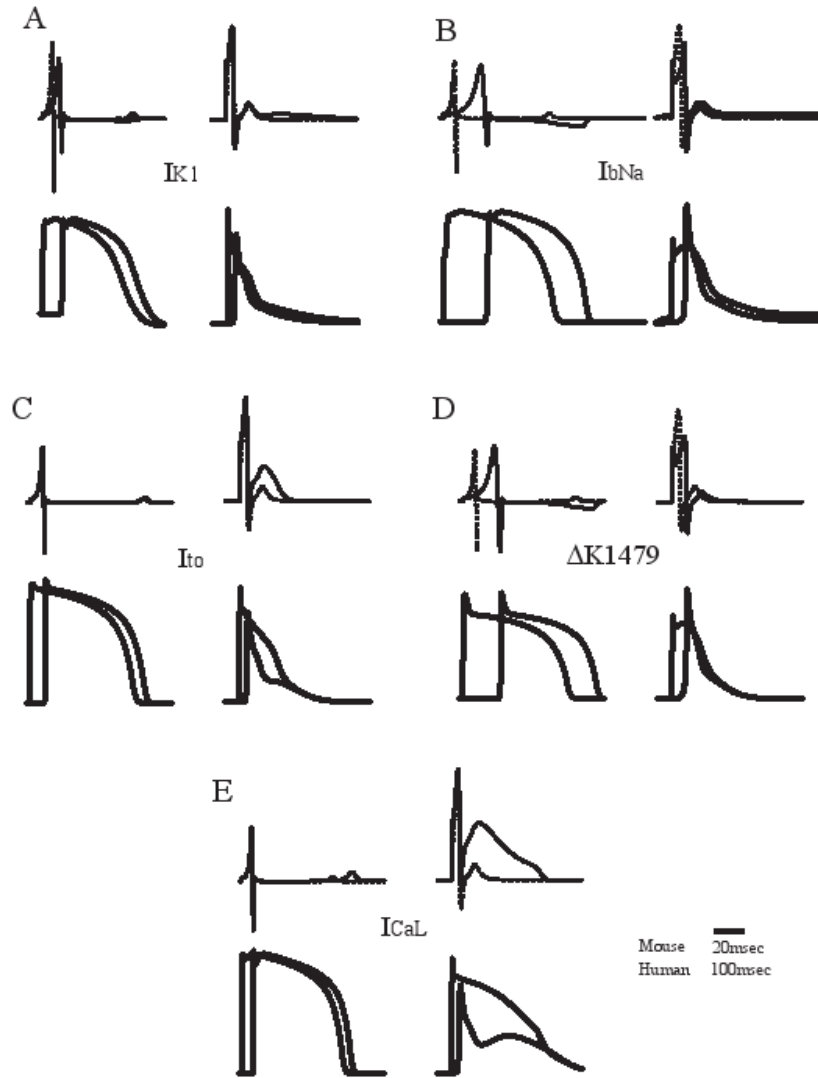


Fig. 3. A comparison of pECG (top) and action potentials (bottom) for human (left) and mouse (right) simulations. Data for each modification is shown in four panel groups. For reference, the dotted traces are the nominal pECG. Action potentials are the first and last in the cable. The time scales for mouse and human data are indicated in the lower right.

pECG after the T-wave. In the mouse the rise in resting potential has little impact on conduction velocity and the a and b waves are only slightly altered. The c-wave on the otherhand is significantly prolonged and broadened as a long-lasting gradient is established between epicardium and endocardium during repolarization.

3.3 Reduced I_{bNa} and I_{Na} Unmasking

I_{bna} is a long lasting inward current that when enhanced leads to a prolongation of the APD and QT interval. In the clinic, this condition is referred to as LQT3 and may be difficult to diagnose because the QT prolongation is relative. To unmask the condition, a Na^+ channel blocker (reduced I_{Na}) is given which widens the QRS in both normal and abnormal patients, but eliminates the isopotential and inverts the T-wave only in patients with LQT3. In our simulations, these behavior were reproduced in the human pECG (Figure 3B). In the mouse, however, the I_{Na} block did change the a wave but did not produce a morphological change in the b or c waves.

3.4 Reduced I_{to}

The transient outward current is present in both the mouse and human but the role played in repolarization is far more significant in the mouse. In the human, I_{to} is responsible for the action potential notch and has a relatively small impact on the APD or ECG (Figure 3C). Blocking I_{to} in the human results in a slight increase in the J-wave and increase in the QT interval. The same simulated block in the mouse leaves early repolarization in epicardial cells unchanged while late repolarization shows a short and low voltage plateau. Endocardial cells, other the otherhand, remain at a considerably higher voltage level throughout repolarization. These findings have been observed experimentally by Guo et al. [26], Barry et al. [3] and Brunner et al. [2]. Both simulated and experimental studies show an increase in amplitude and width of the b and c waves.

3.5 $\Delta K1479$ Mutation

A positive shift in activation or negative shift in inactivation kinetics of I_{Na} can lead to Brugada Syndrome [25]. Similar to LQT3, the disease is unmasked in the clinic by partially blocking I_{Na} . In simulations of the unblocked Brugada mutation, the pECG was similar to the nominal pECG for both the human and mouse (Figure 3D). A 70% I_{Na} block in the human mutation simulation, however, resulted in a "coved" T-wave similar to that observed in patients with Brugada Syndrome. A similar 70% I_{Na} block in the mouse mutation simulation did widen the a wave but did not change the morphology of the b or c waves. Further reduction of I_{Na} did not lead to morphological change until conduction was blocked.

3.6 Increased I_{CaL}

I_{CaL} is an inward current that counteracts repolarization. It is present in both the mouse and the human and has been implicated in a number of interesting phenomenon such as sustaining conduction when I_{Na} is reduced [27], modulating restitution properties and the stability of reentry [28], the genesis of early after-depolarizations (EAD) [29] and the source of Timothy Syndrome (LQT8) [4]. In

the human model, a doubling of I_{CaL} resulted in a delayed T-wave (Figure 3E). The impact on the mouse was an increase in both epicardial and endocardial APD, the appearance of an EAD-like deflection in epicardial cells and a drastic amplitude increase and widening of the c-wave.

3.7 Overexpression of I_{Ks} and I_{Kr} in the Mouse

In the human, a partial block of I_{Ks} and I_{Kr} gave rise to an increased QT interval (not shown), a finding consistent with LQT1 and LQT2 respectively. Although I_{Kr} is present in the mouse, it plays little role in repolarization and is not included in the Pandit et al. model. The addition of the human I_{Ks} and I_{Kr} to the mouse ionic model had virtually no effect on the pECG. Both currents in the human have an impact because they have long time constants that act during the plateau. In the mouse, there is no defined plateau and the neither current has time to play a large role in repolarization. These findings mirror Babij et al. [30] where overexpression of I_{Kr} in the mouse did not generate arrhythmias or ECG abnormalities typically associated with LQT2. Likewise, use of a I_{Ks} blocker in the mouse only had an impact at slow heart rates [5].

4 Discussion

Over the past several decades, the mouse has gained prominence in the cardiac electrophysiology literature as the animal model of choice. The purpose of this paper was to compare normal and abnormal transmural conduction and repolarization in the genesis of the ECG for the mouse and human. The overall findings are: 1) It is possible for the mouse left ventricular wall to sustain gradients large enough to generate the c-wave deflection, 2) The human QRS complex is similar to the a-wave of the mouse and 3) The underlying ionic causes of the T-wave in the human and b and c waves of the mouse are different. These studies highlight the importance of carefully interpreting results from mouse models.

Although it is unclear how deflections in the mouse and human ECG are related, most mouse studies use the clinical PQRST notation. These simulation studies demonstrate that, like the human, the thin mouse ventricular wall is capable of sustaining the APD gradients that give rise to deflections corresponding to repolarization. However, the genesis of the b and c waves in the mouse are due to different ionic currents and APD gradients. These discrepancies have led to a wide variations in mouse ECG measurements in the literature [11,17,22]. To avoid future confusion, the authors suggest the development of a standardized mouse ECG scoring system that is distinct from the human scoring.

The transgenic mouse has helped to uncover some very significant biophysical mechanisms. For example, the impact of knocking out specific connexin isoforms (e.g. gap junctions) [6] have been directly linked to slowed conduction. A mouse model enabled the hypothesized depolarization associated with contact monophasic action potential recordings to be directly measured [9]. Perhaps the most important role for the mouse will be in systematically exploring reentry

initiation, maintenance and breakup [10,11,15]. Although, our simulation studies point out potential problems with studying repolarization diseases and therapies in the mouse, experimental repolarization studies may still yield very significant insights. Such studies can be used to unravel important molecular and cellular level dynamics that are more easily studied in the mouse. It is also possible that the normal mouse may be an ideal model to study human short QT syndrome. An interesting possibility would be to "design" a transgenic mouse in which I_{to} , I_{ss} , I_{Kslow} , I_{CaL} or some combination is modified to achieve a plateau in the mouse [2]. The appearance of this plateau may lead to an isopotential in the mouse ECG and a separation between the b wave and c wave. In this situation, the c-wave may more closely mimic the human T-wave. Therefore, the only caution of these simulations is that the value of functional results lies in the interpretation. The authors therefore propose that the results of mouse studies involving repolarization not be taken at face value, but rather are interpreted using computational or theoretical models.

Although both mouse and human pECG were morphologically similar to experimental ECG, the models presented were for isotropic one dimensional cables. This limitation could be lifted by including the impact of heterogeneous coupling through the wall or coupling via gap junctions [21]. As a further step toward increased realism, whole heart and torso models [31] could incorporate fiber architecture and anatomical features that would allow direct computation of a body surface ECG. It has been proposed [17] that the origin of the mouse c-wave is not a transmural gradient but rather an apex-base or left-right gradient. Furthermore, there is evidence to suggest that some regions of the mouse heart begin to repolarize before other regions have depolarized. A full model of the mouse heart and torso could explore these possibilities. On a cellular level, the impact of drugs and the modeling of diseases could be more accurately simulated using more complex models for I_{ion} [32,33] and non-uniform targeting of different cell types.

The authors anticipate that the mouse will continue to help reveal and validate important biophysical mechanisms and that computer models should and will be used to augment these findings.

Acknowledgments

The authors wish to thank the Bucknell University Research Program, REU program (Grant #PHY-0552790) and Pittsburgh Supercomputing center (Grant #IBN050003P).

References

1. Tamaddon, H.S., Vaidya, D., Simon, A.M., Paul, D.L., Morley, G.E.: High-resolution optical mapping of the right bundle branch in connexin40 knockout mice reveals slow conduction in the specialized conduction system. *Circ. Res.* 87, 929–936 (2000)

2. Brunner, M., Guo, W., Mitchell, G.F., Buckett, P.D., Nerbonne, J.M., Koren, G.: Characterization of mice with combined suppression of I_{to} and $I_{K,slow}$. *Am. J. Physiol Heart Circ. Physiol.* 281, H1201–H1209 (2001)
3. Barry, D.M., Xu, H., Schuessler, R.B., Nerbonne, J.M.: Functional knockout of the transient outward current, Long-QT syndrome, and cardiac remodeling in mice. *Circ. Res.* 83, 560–567 (1998)
4. Salama, G., London, B.: Mouse models of long QT syndrome *J Physiol.* 578, 43–53 (2007)
5. Drici, M., Arrighi, I., Chouabe, C., Mann, J.R., Lazdunski, M., Romey, G., Barhanin, J.: Involvement of *IsK*-associated K^+ channel heart rate control of repolarization in a murine engineered model of Jervell and Lange-Nielsen syndrome. *Circ. Res.* 83, 95–102 (1998)
6. Morley, G.E., Vaidya, D., Samie, F.H., Lo, C., Delmar, M., Jalife, J.: Characterization of conduction in the ventricles of normal and heterozygous Cx43 knockout mice using optical mapping. *J. Cardiovasc Electrophysiol.* 10, 1361–1375 (1999)
7. Doevendans, P.A., Daemen, M.J., de Muinck, E.D., Smits, J.F.: Cardiovascular phenotyping in mice. *Cardiovasc Res.* 39, 34–49 (1998)
8. Berul, C.I.: Electrophysiological phenotyping in genetically engineered mice. *Physiol Genomics* 13, 207–216 (2003)
9. Knollmann, B.C., Tranquillo, J., Sirenko, S.G., Henriquez, C., Franz, M.R.: Microelectrode study of the genesis of the monophasic action potential by contact electrode technique. *J. Cardiovasc Electrophysiol.* 12, 1246–1252 (2002)
10. Vaidya, D., Morley, G.E., Samie, F.H., Jalife, J.: Reentry and fibrillation in the mouse heart: A challenge to the critical mass hypothesis. *Circ. Res.* 85, 174–181 (1999)
11. Nerbonne, J.M.: Studying cardiac arrhythmias in the mouse - a reasonable model for probing mechanisms? *Trends Cardiovasc Med.* 14, 83–93 (2004)
12. Jiang, Y., Pandya, K., Smithies, O., Hsu, E.W.: Three-dimensional diffusion tensor microscopy of fixed mouse hearts. *Magn Reson Med.* 53, 1133–1137 (2004)
13. Punske, B.B., Taccardi, B., Steadman, B., Ershler, P.R., England, A., Valencik, M.L., McDonald, J.A., Litwin, S.E.: Effect of fiber orientation on propagation: electrical mapping of genetically altered mouse hearts. *J. Electrocardiol.* 38(40-4), 40–44 (2005)
14. Nygren, A., Clark, R.B., Belke, D.D., Kondo, C., Giles, W.R., Witkowski, F.X.: Voltage-sensitive dye mapping of activation and conduction in adult mouse hearts. *Annals of BME* 28, 958–967 (2000)
15. Anumonwo, J.M.B., Tallini, Y.N., Vetter, F.J., Jalife, J.: Action potential characteristics and arrhythmogenic properties of the cardiac conduction system of the murine heart. *Circ. Res.* 89, 329–335 (2001)
16. Sampson, K.J., Henriquez, C.S.: Electrotonic influences on action potential duration dispersion in small hearts: a simulation study. *Am. J. Physiol. Heart Circ. Physiol.* 289, 350–360 (2005)
17. Liu, G., Iden, J.B., Kovithavongs, K., Gulamhusein, R., Duff, H.J., Kavanagh, K.M.: In vivo temporal and spatial distribution of depolarization and repolarization and the illusive murine T wave. *J. Physiol.* 555, 267–279 (2003)
18. Pandit, S.V., Clark, R.B., Giles, W.R., Demir, S.S.: A mathematical model of action potential heterogeneity in adult rat left ventricular myocytes. *Biophys. J.* 81, 3029–3051 (2001)
19. ten Tusscher, K.H.W.J., Nobel, D., Nobel, P.J., Panfilov, A.V.: A model for human ventricular tissue. *Am. J. Physiol Heart Circ. Physiol.* 286, H1573–H1589 (2004)

20. Harrild, D., Henriquez, C.: A computer model of normal conduction in the human atria. *Circ. Res.* 87, E25–36 (2000)
21. Gima, K., Rudy, Y.: Ionic current basis of electrocardiographic waveforms: A model study. *Circ. Res.* 90, 889–896 (2002)
22. Danik, S., Cabo, C., Chiello, C., Kang, S., Wit, A.L., Coromilas, J.: Correlation of repolarization of ventricular monophasic action potential with ECG in the murine heart. *Am. J. Physiol.* 283, H372–H381 (2002)
23. Agduhr, E., Stenstrom, N.: The appearance of the electrocardiogram in heart lesions produced by cod liver oil treatment. *Acta Paediatr* 33, 493–588 (1929)
24. Plonsey, R.: The active fiber in a volume conductor. *IEEE Trans. Biomed Eng.* 5, 371–381 (1974)
25. Zhang, Z.S., Tranquillo, J., Neplioueva, V., Bursac, N., Grant, A.O.: Sodium channel kinetic changes that produce Brugada syndrome or progressive cardiac conduction system disease. *Am. J. Physiol Heart Circ. Physiol.* 292, H399–H407 (2007)
26. Guo, W., Li, H., London, B., Nerbonne, J.M.: Functional Consequences of elimination of $I_{to,f}$ and $I_{to,s}$. *Circ. Res.* 87, 73–79 (2000)
27. Shaw, R.M., Rudy, Y.: Ionic mechanisms of propagation in cardiac tissue. Roles of the sodium and L-type calcium currents during reduced excitability and decreased gap junction coupling. *Circ. Res.* 81, 727–741 (1997)
28. Qu, Z., Weiss, J.N., Garfinkel, A.: Cardiac electrical restitution properties and stability of reentry spiral waves: a simulation study. *Am. J. Physiol.* 276, H269–283 (1999)
29. Viswanathan, P.C., Rudy, Y.: Pause induced early afterdepolarizations in the long QT syndrome: a simulation study. *Cardiovasc Res.* 42, 530–542 (1999)
30. Babij, P., Askew, R., Nieuwenhuijsen, B., Su, C., Bridal, T.R., Jow, B., Argentieri, T.M., Kulik, J., DeGennaro, L.J., Spinelli, W., Colatsky, T.J.: Inhibition of cardiac delayed rectifier K⁺ current by overexpression of the Long-QT syndrome HERG G628S mutation in transgenic mice. *Circ. Res.* 83, 668–678 (1998)
31. Tranquillo, J.V., Hlavacek, J., Henriquez, C.S.: An integrative model of mouse cardiac electrophysiology from cell to torso. *Europace* 2, 56–70 (2005)
32. Bondarenko, V.E., Szigeti, G.P., Bett, G.C.L., Kim, S., Rasmusson, R.L.: Computer model of action potential of mouse ventricular myocytes. *Am. J. Physiol. Heart Circ. Physiol.* 287, H1378–H1403 (2004)
33. Iyer, V., Mazhari, R., Winslow, R.: A computational model of the human left-ventricular epicardial myocyte. *Biophys. J.* 87, 1507–1523 (2004)